



Title	Singular-continuous nowhere-differentiable attractors in neural systems
Author(s)	Tsuda, I.; Yamaguchi, A.
Citation	Hokkaido University Preprint Series in Mathematics, 360, 1-24
Issue Date	1996-11-1
DOI	10.14943/83506
Doc URL	http://hdl.handle.net/2115/69110
Type	bulletin (article)
File Information	pre360.pdf



[Instructions for use](#)

**Singular-Continuous
Nowhere-Differentiable Attractors
in Neural Systems**

I. Tsuda and A. Yamaguchi

Series #360. November 1996

HOKKAIDO UNIVERSITY

PREPRINT SERIES IN MATHEMATICS

- #336 Y. Giga, M.E. Gurtin and J. Matias, On the dynamics of crystalline motions, 67 pages. 1996.
- #337 I. Tsuda, A new type of self-organization associated with chaotic dynamics in neural networks, 22 pages. 1996.
- #338 F. Hiroshima, A scaling limit of a Hamiltonian of many nonrelativistic particles interacting with a quantized radiation field, 34 pages. 1996.
- #339 N. Tominaga, Analysis of a family of strongly commuting self-adjoint operators with applications to perturbed Dirac operators, 29 pages. 1996.
- #340 A. Inoue, Abel-Tauber theorems for Fourier-Stieltjes coefficients, 17 pages. 1996.
- #341 G. Ishikawa, Topological classification of the tangent developables of space curves, 19 pages. 1996.
- #342 Y. Shimizu, A remark on estimates of bilinear forms of gradients in Hardy space, 8 pages. 1996.
- #343 N. Kawazumi and S. Morita, The primary approximation to the cohomology of the moduli space of curves and cocycles for the stable characteristic classes, 11 pages. 1996.
- #344 M.-H. Giga and Y. Giga, A subdifferential interpretation of crystalline motion under nonuniform driving force, 18 pages. 1996.
- #345 A. Douai and H. Terao, The determinant of a hypergeometric period matrix, 20 pages. 1996.
- #346 H. Kubo and K. Kubota, Asymptotic behaviors of radially symmetric solutions of $\square u = |u|^p$ for super critical values p in even space dimensions, 66 pages. 1996.
- #347 T. Nakazi and T. Yamamoto, Weighted Norm Inequalities For Some Singular Integral Operators, 17 pages. 1996.
- #348 Y. Ito and I. Nakamura, Hilbert schemes and simple singularities A_n and D_n , 22 pages. 1996.
- #349 R. Agemi and K. Yokoyama, The null condition and global existence of solutions to systems of wave equations with different speeds, 42 pages. 1996.
- #350 F. Hiroshima, Weak coupling limit with a removal of an ultraviolet cut-off for a Hamiltonian of particles interacting with a massive scalar field, 21 pages. 1996.
- #351 T. Nakazi and Y. Watatani, Invariant subspace theorems for subdiagonal algebras, 22 pages. 1996.
- #352 Y. Nishiura and H. Suzuki, Nonexistence of stable turing patterns with smooth limiting interfacial configurations in higher dimensional spaces, 21 pages. 1996.
- #353 Y.-G. Chen, Y. Giga and K. Sato, On instant extinction for very fast diffusion equations, 9 pages. 1996.
- #354 A. Gyoja and H. Yamashita, Associated variety, Kostant-Sekiguchi correspondence, and locally free $U(n)$ -action on Harish-Chandra modules, 25 pages. 1996.
- #355 G. Ishikawa, Topology of plane trigonometric curves and the strangeness of plane curves derived from real pseudo-line arrangements, 18 pages. 1996.
- #356 N.H. Bingham and A. Inoue, The Drasin-Shea-Jordan theorem for Hankel transforms of arbitrarily large order, 13 pages. 1996.
- #357 S. Izumiya, Singularities of solutions for first order partial differential equations, 20 pages. 1996.
- #358 N. Hayashi, P.I. Naumkin and T. Ozawa, Scattering theory for the hartree equation, 14 pages. 1996.
- #359 I. Tsuda and K. Tadaki, A logic-based dynamical theory for a genesis of biological threshold, 49 pages. 1996.

Singular-Continuous Nowhere-Differentiable Attractors in Neural Systems

Ichiro Tsuda and Akihiro Yamaguchi†

Applied Math. and Complex Systems Research Group,

Department of Mathematics,

Graduate School of Science,

Hokkaido University,

Sapporo, 060 Japan

†Research Group of Complex Systems Engineering,

Faculty of Engineering,

Hokkaido University,

Sapporo, 060 Japan

Aknowledgments

One of the authors (I. T.) would like to express his special thanks to Otto Rössler, Gerold Baier, Axel Hoff and Hans Diebner for their invaluable discussions. He also thanks Reimara and Michal Rössler for encouragement. This work was partially supported by Grant-in-Aid #08279103 for Scientific Research on Priority Areas on "System Theoretical Understandings for Brain Higher Functions," the Ministry of Education, Science, Sports, and Culture of Japan.

Ichiro Tsuda, Department of Mathematics, Graduate School of Science, Hokkaido University, Sapporo 060, Japan; tel: 81-11-706-3824; fax: 81-11-727-3705; e-mail:tsuda@math.hokudai.ac.jp, to whom correspondence should be addressed.

Running title: SCND attractors

Abstract

We present a neural model for a singular-continuous nowhere-differentiable (SCND) attractors. This model shows various characteristics originated in attractor's nowhere-differentiability, in spite of a differentiable dynamical system. SCND attractors are still unfamiliar in the neural network studies and have not yet been observed in both artificial and biological neural systems. With numerical calculations of various kinds of statistical quantities in artificial neural network, dynamical characters of SCND attractors are strongly suggested to be observed also in neural systems experiments. We also present possible information processings with these attractors.

Key words: Singular-continuous nowhere-differentiable attractors; Chaos-driven contraction dynamics; Information processings on Cantor set; Dimension gap.

1 Introduction

Dynamical states in neural systems can be represented by various kinds of attractors in dynamical systems: a stationary state by fixed point, a periodically oscillatory state by limit cycle, a quasi-periodic state by torus, a low-dimensional chaotic state by strange attractor, and a high-dimensional itinerant state by itinerant attractor. Among others, recently an itinerant attractor has been highlighted in the research of complex systems like neural systems, where the new notion of chaotic itinerancy was proposed. (Ikeda *et al*, 1989; Kaneko, 1990; Tsuda, 1991a; 1991b). These states have been widely investigated and also observed in experiments (for epoch-making experimental works including chaotic itinerancy in neural systems, see Freeman, 1987; 1994; 1995a; 1995b; Skarda and Freeman, 1987; Kay *et al*, 1995). There is still, however, another dynamical attractor which was named "strange nonchaotic attractor" by Grebogi, Otto, Kaplan and Yorke (Kaplan & Yorke, 1979; Kaplan *et al*, 1984; Grebogi *et al*, 1984). Here, "strange" means the presence of Cantor sets, and "nonchaotic" the absence of positive Lyapunov exponents.

A possible mechanism of strange nonchaotic attractors was recently proposed by Rössler *et al* (1992). Actually, the attractors can be represented by singular-continuous nowhere-differentiable (SCND) functions. We will provide the definition of this class of functions in §3, where we will develop a theory to explain "strange" dynamic characters of our model neural network. It should, however, be noted that SCND attractors must be, in general, different from strange nonchaotic attractors since the former appears in contraction subspace of a whole space including chaotic components, whereas the latter does not include chaotic components ¹.

Any theories, models, and even experimental observations for this attractor in neural systems have not reported so far, except that we showed the presence of such an attractor in neural networks (Tsuda, 1996). Furthermore, the questions have not yet been elucidated if this attractor could be observed in biological neural networks, and also if it could subserve the information processings in brain. In this paper, we present a small scale neural network

¹Rössler, private communication

model which exhibits SCND attractors. Our aim is to elucidate the former question and for the latter to present hypotheses based on the numerical simulations of the model.

A neural network model exhibiting SCND attractors will be presented in §2. In §3, a general scheme giving rise to SCND attractors will be addressed, whereby the mechanism of SCND attractors obtained in §2 will be elucidated. In §4, various characteristics of the obtained SCND attractors will be studied. Section 5 will be devoted to conclusion and discussion, where hypotheses on information processings with SCND attractors and the possibility of the observation of SCND attractors in biological neural networks will be addressed.

2 A model

Our model neural network presented here is of a small scale. The model consists of only three neurons, two of which are called here a "static" neuron and the other one a "dynamic" neuron. A static neuron's activity eventually relaxes to stationary firings which is represented by a fixed point in phase space, whereas a dynamic neuron fires chaotically, thus it is represented by chaotic attractor. It would be convenient to use a chaotic neuron model introduced by Aihara *et al* (1990) in order to model both static and dynamic neurons in terms of a family of chaotic map.

We adopt here an mutually interacting static neurons: one is supposed to be excitatory and the other inhibitory. Suppose a dynamic neuron which is supposed to be excitatory drives both static neurons. This condition of the model is natural, because one can easily conceive the biological situation that a chaotic neuron or a chaotic neuron assembly drives a static neuron or a static neuron assembly. We control interacting static neurons to form a contraction map. Hence the present system belongs to a class of chaos-driven contraction maps. The model equations are as follows.

$$x_{n+1} = f_1\left(-\sum_{r=0}^n b_1^r x_{n-r} + I\right), \quad (1)$$

$$y_{n+1} = f_2\left(-\sum_{r=0}^n b_2^r y_{n-r} + c_{zy} z_n + c_{xy} x_n\right), \quad (2)$$

$$z_{n+1} = f_2\left(-\sum_{r=0}^n b_3^r z_{n-r} + c_{yz}y_n + c_{xz}x_n\right), \quad (3)$$

where $0 < b_1, b_2, b_3 < 1$, c_{uv} are a synaptic strength from neuron u to v and $c_{zy} < 0$, $c_{yz}, c_{xy}, c_{xz} > 0$. The functions $f_i(x)$ ($i = 1, 2$) is a sigmoidal function described as follows.

$$f_i(x) = \frac{1}{1 + e^{-\gamma_i x}}, \quad (i = 1, 2). \quad (4)$$

In the simulation, $\gamma_1 = 70$ and $\gamma_2 = 1.5$ were fixed in order to assure the chaos-driven contraction map.

This system looks dependent on a whole history of states, but actually it can be reduced to the dynamical system of six-dimension if the terms of history-dependent internal states are replaced by one variable each. Let us perform the replacement of variables such that $X_n \equiv -\sum_{r=0}^n b_1^r x_{n-r} + I$, $Y_n \equiv -\sum_{r=0}^n b_2^r y_{n-r} + c_{zy}z_n + c_{xy}x_n$, and $Z_n \equiv -\sum_{r=0}^n b_3^r z_{n-r} + c_{yz}y_n + c_{xz}x_n$. Then, the reduced model equations are as follows.

$$X_{n+1} = b_1 X_n - f_1(X_n) + \alpha, \quad (5)$$

$$Y_{n+1} = b_2 Y_n - f_2(Y_n) + c_{zy}(f_2(Z_n) - b_3 f_2(Z'_n)) + c_{xy}(f_1(X_n) - b_1 f_1(X'_n)), \quad (6)$$

$$Z_{n+1} = b_3 Z_n - f_2(Z_n) + c_{yz}(f_2(Y_n) - b_2 f_2(Y'_n)) + c_{xz}(f_1(X_n) - b_1 f_1(X'_n)), \quad (7)$$

$$X'_{n+1} = X_n, \quad (8)$$

$$Y'_{n+1} = Y_n, \quad (9)$$

$$Z'_{n+1} = Z_n, \quad (10)$$

where $\alpha = I(1 - b_1)$. The last three variables, X' , Y' , and Z' simply give a linear effect, in particular, $X'_n - X_n$ plane defines just one-dimensional map $X_{n+1} = F(X_n)$, where $F(X_n) = b_1 X_n - f_1(X_n) + \alpha$. Figure 1 shows a map of a static neuron ((a)) and a dynamic one ((b)) when each is isolated.

-Fig.1 (a) and (b)-

The parameters b_1 , b_2 , and b_3 are a measure of volume contraction. Throughout the present study, we assume that $b \equiv b_1 = b_2 = b_3$. We will see, in §4, the effect of this parameter values to the dimensionality.

Let us see the dynamics on the cross section $X = \text{constant}$, for instance, $X = 0.05 (\pm 0.0005)$, which provides two values for variable X' , whereby two branches of Cantor set appears on the section (Fig.2(a)–(c)). If the cross-section is taken as $X = X^s$, where $F(X^s) \in [F^2(X_l^*), F^2(X_r^*)]$, only one branch of Cantor set is seen. Here X_l^* and X_r^* denotes the left and the right critical points of the map F , respectively, *i.e.* $dF(X_l^*)/dX = dF(X_r^*)/dX = 0$. As seen in Fig.2, an attractor becomes fat due to an increase of parameter b , namely an decrease of contraction rate. Figure 3 indicates a return map of Y variable only on the cross section, where Cantor structure is clearly seen. This is a reflection of attractor's Cantor structure. It turns out by the dimension study (see §4) that at this parameter value $b = 0.93$, the attractor dimension is less than unity on the cross-section, though in the return map it looks higher than unity. This indicates that the Cantor structure constructed on at least two-dimensional space.

–Fig.2(a), (b) and (c)–

–Fig.3–

The cross section was chosen not to see chaotic components, thereby what we see is a contraction space. Thus, on this section one can see the details of Cantor structure of the attractors, whereas the details of Cantor set in usual chaos in low dimensional flow are difficult to be seen. With the theory provided in the next section, the reason why these attractors belong to the class of singular-continuous nowhere-differentiable attractors will be elucidated.

3 Singular-continuous nowhere-differentiable attractors

3.1 Continuous but nowhere-differentiable functions

Continuous but nowhere-differentiable functions have been widely investigated (Takagi, 1973; Titchmarsh, 1985; Hata, 1988a; 1988b; 1994). In particular, Yamaguti (1989), and

Yamaguti and Hata (1984) elucidated a relation between fractals (Mandelbrot, 1982) and chaos. Recently, perhaps the simplest example of this class of functions has been proposed by Katsuura (1991). Katsuura's function (named by Rössler) is obtained from the graph of asymptotic form of unit square transformed by a specific contraction mapping. The following Katsuura map defines a contraction of any subset of the unit square $D = [0,1] \times [0,1]$ when an appropriate metric is introduced.

Let us define contraction mappings $K_i: D \rightarrow D$ ($i = 1, 2, 3$).

$$K_1(x, y) = \left(\frac{x}{3}, \frac{2y}{3}\right), \quad (11)$$

$$K_2(x, y) = \left(\frac{2-x}{3}, \frac{1+y}{3}\right), \quad (12)$$

$$K_3(x, y) = \left(\frac{2+x}{3}, \frac{1+2y}{3}\right) \quad (13)$$

Each of these mappings has a fixed point, $(0,0)$, $(\frac{1}{2}, \frac{1}{2})$, and $(1,1)$, respectively. Here, let $H(D)$ be a collection of all nonempty closed subsets of D . For every $A \in H(D)$,

$$K(A) := K_1(A) \cup K_2(A) \cup K_3(A). \quad (14)$$

For every $A, B \in H(D)$, the Hausdorff metric is defined.

$$d_H(A, B) := \inf\{\epsilon > 0 \mid N_\epsilon(A) \supset B \text{ and } N_\epsilon(B) \supset A\}, \quad (15)$$

where $N_\epsilon(\bullet)$ is an ϵ -neighborhood of \bullet . Then, K is a contraction mapping on $H(D)$ under this metric.

Let $L_0 = (x, x) \in D$ and $L_n = K(L_{n-1})$, then L_n is a graph of continuous function $f_n : [0,1] \rightarrow [0,1]$. In particular, a continuous function $f_\infty : [0,1] \rightarrow [0,1]$ exists. The mapping K has a unique fixed point L^* in $H(D)$, since K is a contraction mapping on $H(D)$. Therefore, for any $A \in H(D)$, a series $\{K^n(A)\}$ converges to L^* with respect to the metric d_H . Then, L^* is a graph of f_∞ , namely L_n converges to L^* . Katsuura (1991) proved with a standard analysis that the function f_∞ is nowhere-differentiable on $[0,1]$, here differentiability includes convergence even to plus or minus infinity.

3.2 Singular-continuous nowhere-differentiable functions

Rössler *et al* (1992) constructed a singular-continuous but nowhere-differentiable function, based on Katsuura's function. A singular continuity is a continuity on Cantor set. We here present a definition of singular continuity, and differentiability on Cantor set. A possible definition is as follows.

Definition: Singular Continuity

Define a finite set of continuous functions $h_n^{(i)}(x)$ on each subinterval $I_n^{(i)}$ at each finite step n as constructing Cantor set in such a way that $\lim_{x \uparrow \alpha_n^{(i)}} h_n^{(i)}(x) = \lim_{x \downarrow \beta_n^{(i)}} h_n^{(i)}(x)$, where open subintervals $(\alpha_n^{(i)}, \beta_n^{(i)})$ are removed ones in the construction of Cantor set as a support. If this process continues to infinity, then a singular continuous function is defined as $\{h_\infty^{(i)}(x)\}_i$, $x \in$ Cantor set, $(i = 1, 2, \dots, \infty)$.

Definition: Differentiability on Cantor Set

Define a continuous function $h_n^{(i)}(x)$ on each subinterval $I_n^{(i)}$ at each finite step n as constructing Cantor set. For each subinterval $I_n^{(i)} = [a_n^{(i)}, b_n^{(i)}]$, a quotient $\delta_n^{(i)} \equiv \frac{h_n^{(i)}(b_n^{(i)}) - h_n^{(i)}(a_n^{(i)})}{b_n^{(i)} - a_n^{(i)}}$ is defined. There exists a collection of functional series, one of which is denoted by $\{\delta_k\}_k$, that accords to a respective series of subintervals $\{J_n\}$ whose one end point is an element of Cantor set and the other end point monotonously converges to that element. If every functional series converges, including $\pm \infty$, then a function $\{h_\infty^{(i)}(x)\}_i$, $x \in$ Cantor set, $(i = 1, 2, \dots, \infty)$ is differentiable on Cantor set.

Since this is a definition by Dini's derivatives D (for example, Titchmarsh, 1985), several definitions are possible, each expressing a different degree of differentiability. Namely,

a) weak differentiability: $D^+ = D_+$, or $D^- = D_-$.

b) strong differentiability: $D^+ = D_+ = D^- = D_-$.

A typical example of singular-continuous nowhere-differentiable function has been introduced by Rössler *et al* (1992), which is given by the following equations:

$$R_1(x, y) = \left(\frac{x}{5}, \frac{2y}{3}\right), \quad (16)$$

$$R_2(x, y) = \left(\frac{3-x}{5}, \frac{1+y}{3}\right), \quad (17)$$

$$R_3(x, y) = \left(\frac{4+x}{5}, \frac{1+2y}{3} \right). \quad (18)$$

For any $A \in H(D)$, define

$$R(A) := R_1(A) \cup R_2(A) \cup R_3(A). \quad (19)$$

This gives a contraction mapping under the Hausdorff metric ¹⁵(12), hence S_n recursively defined by $S_n = R(S_{n-1})$ for given $S_0 = (x, x)$ is a graph of the function g_n on $[0,1]$. In particular, the graph S_∞ of g_∞ consists of isolated points, and g_∞ is singular-continuous nowhere-differentiable.

3.3 Dimensionality

Let us estimate, according to Rössler *et al* (1992), the dimensions of S_∞ derived from the above Rössler's model. For the first time, it is obvious that the topological dimension $\dim_t(S_\infty) = 0$. On the other hand, the Hausdorff dimension $\dim_h(S_\infty)$ is simply estimated by using the self-similarity such that $\dim_h(S_\infty) = \frac{\log \frac{25}{3}}{\log 5} = 1.317 \dots$. Namely,

$$\dim_h(S_\infty) - \dim_t(S_\infty) > 1.0. \quad (20)$$

On the other hand, the dimensions of the graph of Katsuura's function f_∞ which is 'simply' nowhere-differentiable are $\dim_t(L_\infty) = 1$ and $\dim_h(L_\infty) = \frac{\log 5}{\log 3} = 1.4649 \dots$, hence

$$\dim_h(L_\infty) - \dim_t(L_\infty) < 1.0. \quad (21)$$

The above two models, (11) \sim (13) and (16) \sim (18), are not dynamical systems but simply contraction mappings. Our interest here is an attractor of differentiable dynamical systems, which can be represented by nowhere-differentiable or singular-continuous nowhere-differentiable functions. An attractor represented by the Weierstrass function was discussed by Moser (1969) in the context of structural stability. Recently, Kaneko has found a similar model exhibiting a fractal torus (Kaneko, 1986). A singular-continuous nowhere-differentiable attractor was first found by Yorke *et al* (Greboji *et al*, 1984; Kaplan and Yorke, 1979), which was named strange nonchaotic attractors. Actually, Rössler *et al* (1992)

have proposed the singular-continuous nowhere-differentiable function discussed above as a mechanism of strange nonchaotic attractors, and proposed another models (Rössler and Hudson, 1984) of this class, where the name "superfat attractors" was given. According to Rössler, the eqn.(20) should generally hold for singular-continuous nowhere-differentiable attractors. This means that the Rössler model, (16) \sim (18), provides a ground for the Kaplan-Yorke conjecture (Kaplan and Yorke, 1979) that a dimension of chaotic attractors can exceed its topological dimension by more than unity. This can happen by the presence of negative Lyapunov exponents whose absolute values are smaller than positive exponents, as seen in neuro-chaotic itinerancy (Tsuda *et al*, 1987; Tsuda, 1991a; 1991b; 1992; 1994). In order to establish this condition for the present neural model, the contraction parameter b should be close to unity. As in §4, it can be realized in larger values than around $b = 0.95$.

3.4 An example of dynamical system exhibiting singular-continuous nowhere-differentiable attractors

The following dynamical system, which is so called Axiom A system, shows SCND attractor, typically in case of $a=9.0$, $b=0.3$, and $c=0.7$ (Rössler *et al*, 1995).

$$x_{n+1} = ax_n \pmod{2\pi}, \quad (22)$$

$$y_{n+1} = by_n - c \cos(ax_n), \quad (23)$$

$$z_{n+1} = bz_n + c \sin(ax_n), \quad (24)$$

$$w_{n+1} = bw_n - c \sin(2 \times ax_n). \quad (25)$$

This is one of the typical chaos-driven contraction mappings. One can see SCND attractor on the cross section $x=\text{constant}$. Lyapunov spectrum of this system is (2.197, -1.204, -1.202, -1.204), thus the Lyapunov dimension, which is equivalent to the Hausdorff dimension in this case, is $\dim_\lambda = 2.825$. On the other hand, the topological dimension is $\dim_t = 1.0$, since volume is contracted in all of three directions than x -coordinate, where only a set of isolated points is eventually formed. Hence the same inequality as in (20) holds. This relation of dimensions means that the attractor is sparsely distributed in phase

space. This may provide a merit for information processings with Cantor coding (Siegelmann & Sontag, 1994). On the details of three dimensional Cantor set in this Axiom A system, see Rössler *et al* (1995) and Tsuda (1996).

4 Dynamic features of neuro-SCND attractors

In order to characterize the attractor seen on the cross-section, we calculated the following statistical quantities: invariant measure, Lyapunov spectrum, mutual information, entropies, distribution of recurrence time, and dimension. The quantities except for the Lyapunov spectrum and dimension were calculated with some partition, thus giving coarse-grained ones. We changed partition in several systematic ways, and concluded the presence of invariant characters. We also investigated a noise effect for entropies and mutual information. We report these issues in detail.

1. Invariant measure

Invariant measure was computed in Y - Z plane, using orbits found on the cross section, $X = \text{constant}$. As seen in Fig. 4, where the plane was divided by 30×30 , the density becomes very high at each one boundary of coarse-grained Cantor set, and decays drastically as it goes to the other end. This feature is self-similarly embedded in each subset (not shown in the figure).

—Fig.4—

This singularity other than self-similarity stems from the singularity of the invariant density of driving chaotic neuron. The invariant measure of the isolated chaotic neuron is roughly estimated as follows. Let X_r^* and X_l^* be the right and the left critical points of the map, respectively, and let $\tau(X_r^*, X)$ and $\tau(X_l^*, X)$ be time steps of orbit arriving at X , starting from the right and the left critical points, respectively. We take into account only the critical points for the singularity of invariant measure, since the map is almost piecewise-linear. Furthermore, the slope b is close to but less than unity. Hence, $\tau(X_r^*, X)^{-1}$, or $\tau(X_l^*, X)^{-1}$ can give a rough estimation of this kind of singular invariant

measure². Which quantity $\tau(X_r^*, X)^{-1}$ or $\tau(X_l^*, X)^{-1}$ is more effective than the other depends on the shift value $f(0)$. Fig. 5 (a), (b), and (c) show an invariant measure of the chaotic map, $\tau(X_r^*, X)^{-1}$, and $\tau(X_l^*, X)^{-1}$, respectively. It turns out that the invariant measure is approximated by $\tau(X_r^*, X)^{-1}$ in this case.

–Fig.5 (a), (b), and (c)–

Moreover, let us calculate a distribution of a recurrence time of orbits starting from points in $X \pm \Delta X$. The following exponent ν does not depend on this precision. Since X is a driving force, this distribution is equivalent to that of the neural net concerned, namely the distribution of recurrence time on the cross section $X(\pm \Delta X)$. At each cross section X , it was numerically observed that the distribution follows the relation,

$$P_X(T) = A(X) \exp(-\nu(X)T) \quad (T \leq T_{max}(b)), \quad (26)$$

where T is recurrence time. It should be noted that recurrence time has upper bound, T_{max} which depends on the contraction parameter b . The larger the value of b is, the longer is the upper bound up to infinity in the conservation limit $b = 1$. In Fig.6, we plot the exponent $\nu(X)$ as a function of the cross section X . This resembles the invariant measure of isolated chaotic neuron map, especially the positions of singularity completely coincide with each other. This relation between $\nu(X)$ and invariant measure was first found here. From dynamical systems viewpoint, it is valuable to study whether this is a universal character in chaotic dynamical systems or specific only to almost piecewise-linear systems. This is here left as an open question.

–Fig.6–

Recurrence time T may also approximate the period of unstable periodic orbits which lie in the neighborhood of the wandering orbits with such recurrence time. According to Kai and Tomita (1980), the invariant measure of chaos is determined by a sum of weights

²This was actually predicted by Yoichiro Takahashi (personal communication)

of periodic orbits, here weight is inversely proportional to an absolute value of the product of derivatives of map at those periodic points. The present relation (26) is thus qualitatively explained by Kai and Tomita theory, though quantitative derivation is not straightforward.

Rewriting the relation (26), an explicit expression of $\nu(X)$ is

$$\nu(X) = -T^{-1} \ln P_X(T) + T^{-1} \ln A(X). \quad (27)$$

If one can view the recurrence time as the period of periodic orbit in the above sense, the integral of $P_X(T)$ with respect to X could provide a total number of periodic points of period T , here denoted by $P(T)$. Then, topological entropy is given by $\lim_{T \rightarrow \infty} T^{-1} \ln P(T)$. Thus, the first term on the right hand side of (26) may represent a local "density" of topological entropy, that is, a local topological complexity of the map of T times iteration, though opposite sign. On the other hand, $A(X)$ is proportional to $\nu(X)$, hence the second term could represent roughly a local entropy, that is, a local information created per iteration. Thus, here an information is roughly a sum of invariant measure and local topological complexity.

The singularity of this forcing measure directly influences the singularity of invariant measure on the cross section in case of network. The self-similarity of measure on the section directly stems from the singular-continuous nowhere-differentiability of the attractor.

2. Lyapunov spectrum and dimension

We computed Lyapunov spectrum from which Lyapunov dimension is derived. In the present model, only one dimension formed by one-dimensional chaotic map in $X' - X$ space results in the presence of positive Lyapunov exponent, since other variables are responsible for contraction, giving rise to negative Lyapunov exponents. Depending on b , the absolute value of some negative exponents can be smaller than the positive one, which gives rise to the dimension gap discussed in §3. In Fig.7, the Lyapunov dimension is shown for each value of b . In Table 1, Lyapunov spectrum and dimension are shown for some typical values of b . For some values of b , dimension is low, that indicates the occurrence of bifurcations. Except for these values, the dimension increases as b increases. On the other hand, the contraction subsystem forced by the chaotic orbits with arbitrarily high period makes zero-

dimension only (Hirsch and Smale, 1974; Rössler and Hudson, 1984). Thus, topological dimension is unity over a whole range of parameter $b(< 1)$, inherited from one-dimensional chaotic component. At around $b = 0.95$, the dimension gap is more than unity, and it is more than two at around $b = 0.99$.

–Fig.7–

–Table 1–

This dimension gap may provide a merit for information processing on Cantor set. Since one must usually process information in noisy environments, the question becomes important how the noise can be effectively reduced. The dimension gap means that attractor is distributed in the space dimension. If one encodes information on the distributed Cantor elements, one can discriminate the errored codes from real codes, since all the errored codes could be in the Cantor gaps. On the other hand, the present system pulls back the disturbed orbits into Cantor set, since the dynamics on the cross section is contractive. Thus, it is also used for an automatic reduction of noise.

3. Entropies

We computed a conditional entropy on the cross section which may approximate the K-S entropy. The conditional entropy is defined as follows:

$$H(U'/U) = - \sum_{i,j} p_i p_{ij} \log p_{ij}, \quad (28)$$

$$= - \sum_{i,j} p(i,j) \log p(i,j)/p_i, \quad (29)$$

where U' and U denote the states on the cross section, p_i a stationary probability distribution, p_{ij} a conditional probability distribution from state $i \in U$ to $j \in U'$, and $p(i,j)$ a simultaneous probability distribution. A various size of bin (dy, dz) was adopted, and the following characteristics was concluded as an invariant one.

Interesting noise effect was found, using a uniform noise. Increasing the noise amplitude, the entropy decreased in some noise range, and increased after some critical point. This

is shown in Fig.8. In order to check if the computed results are reliable, we estimated the number of bins including at least one data point, which is shown in Fig.9. As figure shows, the number of bins increases drastically, that is, the number of data in each bin decreases drastically at the range where entropy abruptly increases, which gives rise to a poor statistical estimation. Hence, we concluded that the decrease of entropy by noise is statistically reliable, but unreliable for the increase phase. Actually, for a reliable range of noise the number of data in each bin is more than ten, which assures a plausible statistical estimation.

–Fig.8–

–Fig.9–

In order to check whether or not this noise effect is an inherent character of SCND attractors, we computed the entropy by changing the size of bin. Consequently, the numerical results did not change qualitatively, especially for the noise level for the minimum value of entropy. The decrease of entropy by noise indicates that noise does not necessarily blur the attractor's Cantor-like structure, and on the contrary to usual diffusion process by noise a more ordered state is created, or extracted by noise from the original attractor. In general, noise plays two roles in such a way that it makes distinct orbits merge into a bin, and on the other hand it makes indistinguishable orbits in bin distribute to some other bins. The former is responsible for a decrease of entropy, but the latter is for an increase of entropy.

In the case of so called noise-induced order (Matsumoto and Tsuda, 1983) observed in chaos, the former effect wins the latter due to the nonuniformity of Markov partitions that provides a variety of inherent orbits. In the present case, it is hard to determine the Markov partition, so that one cannot compare a true orbit with a noisy orbit.

It is, however, possible to conceive the mechanism of the "noise reduction" by noise. In SCND attractor, many to many correspondence among orbits is permitted only on the Cantor set, and almost one to one correspondence holds on empty space (Cantor gap). Here the notion of correspondence among orbits is derived since we observe the orbits only on

the cross section $X = \text{constant}$. Even if the orbits are moved by noise to empty space, the orbits easily come back to the vicinity of the original Cantor element due to the convergent dynamics, as far as the noise is not so large. It may trigger the entropy reduction. Thus, one may call the present noise effect a noise-induced order, though chaotic component is deleted in the present case. This effect is much larger for the activities of inhibitory neuron (Z variable) than the excitatory neuron (Y variable). Actually, the Cantor structure is still visible in inhibitory neuron even when external noise is applied. These features may assure an observability of SCND attractors in biological neural systems. This point will be discussed below in more details.

4. Mutual information

Mutual information is defined by the difference between entropy and conditional entropy. The numerical fact that the invariant distribution and the transition probability distribution are almost equivalent derives the time-invariance of mutual information with a small value depending on the cross section and its precision for the determination. There are some probabilities that a few digits become different between the invariant distribution and the transition probability distribution. These digits contribute to a non-zero value of the mutual information, which differs from the asymptotic case of mutual information in chaos, where zero value is achieved. It turns out in the following way where this non-zero value stems from.

The definition of time-dependent mutual information is as follows (Matsumoto and Tsuda, 1985; 1987; 1988):

$$I(t) = \sum_i p_i \log p_i^{-1} - \sum_i \sum_j p_i p_{ij}(t) \log p_{ij}(t)^{-1}, \quad (30)$$

where t is a discrete time with a measure only on the cross section, p_i a stationary probability distribution of i -th state, and p_{ij} a transition probability distribution from i to j .

In the present case, $p_{ij}(t) = \text{const.}$ w.r.t. t , denoting here q_{ij} . The following equations are empirically obtained.

$$q_{ij} = q_j, \quad (31)$$

$$q_j = \begin{cases} p_j & (\text{for almost all } j) \\ 0 & (\text{otherwise}) \end{cases} \quad (32)$$

Then,

$$I(t) = \sum_i p_i \log p_i^{-1} - \sum_i p_i \sum_j q_{ij} \log q_{ij}^{-1}, \quad (33)$$

$$= \sum_i p_i \log p_i^{-1} - \sum_j q_j \log p_j^{-1}, \quad (34)$$

$$= \sum_i (p_i - q_i) \log p_i^{-1}. \quad (35)$$

The difference between both distributions p_i and q_i lies only in some sites. Let $\Delta_i \equiv p_i - q_i$, denoting missing information in each site i . Then we obtain the following equation.

$$I(t) = \sum_i \Delta_i \log \Delta_i^{-1} = \text{const.} \equiv I. \quad (36)$$

Since Δ_i represents a "missing bit", mutual information here is an information shared between missing bits. This value of I depends on the position of cross section and observation precession. It should be noted that I does not, in general, equal to zero, whereas the zero value is asymptotically achieved in case of chaos.

In Fig.10, the noise effect on mutual information is shown. Here, a similar behavior is seen to the case of conditional entropy. Namely, the non-zero value I does not vary as increasing the noise level up to some level which is around 1/1000 of the system size. Further increase of the noise level by around one digit shows abrupt decrease of I . By the reason from statistical inference, the increase phase of I is not reliable, similarly to the case of conditional entropy.

-Fig.10-

5 Conclusion and discussion

We proposed a neural network model exhibiting singular-continuous nowhere-differentiable (SCND) attractors. This is the first finding of SCND attractors in neural systems. We also elucidated a mechanism of SCND attractors with a help of Rössler's construction of singular-continuous nowhere-differentiable functions. In order to characterize SCND attractors, we calculated invariant measure, Lyapunov dimension in terms of Lyapunov spectrum, entropies, and mutual information. Here, all calculations were performed on the cross section $X = \text{const.}$ Three main features were extracted. First, invariant measure shows a singularity on each coarse-grained element of Cantor set, which stems from the singularity due to a critical point of isolated chaotic neuron map. Second, SCND attractors can possess a dimension gap, namely the Lyapunov dimension can exceed the topological dimension by more than unity. In the present model, we found that the dimension gap increases as the volume contraction parameter b is increased up to unity, except for bifurcation points. Here the maximum dimension gap was 2.08. Third, the statistical quantities like entropies and mutual information is robust for noise up to around 1/1000 of system size in amplitude, and for a bit larger noise they abruptly decrease. Even changing a mesh size for finite computation, this tendency did not change. This indicates the existence of structure inherent in SCND attractors to absorb the external noise. This characteristics would be important in studying information processings of brain with SCND attractors.

Referring to the last formula of mutual information, one may conceive two kinds of information processings on Cantor set. One is the localization of information on Cantor set, and the other the concurrent process of write-in ("learning") and read-out ("retrieval"). The information can be distributed on subsets of Cantor set, but information can never flow among any subsets. This is, however, different from zero-information flow seen in stationary distribution of chaos. In the present case, only the shared information is the information that "missing bits" possess, whose bits provide the difference between invariant measure and transition probability distribution.

On the other hand, the concurrent process emerges as a microscopic mechanism of the sta-

tionarity. In general, in dynamical systems, an expanding map assures a read-out process of information, whereas a contraction map assures a write-in process. In usual chaotic dynamics, an expanding and a contracting phase appears successively, associated with its dynamics. In the present case, these phases progress concurrently, because of chaos-driven contraction mapping. A simpler alternative to conceive this process would be a dissipative baker's transformation. But, in such a case, attractor is constituted by one-dimensional Cantor set, hence singular-continuous nowhere-differentiable functions cannot be constructed.

If the present model is adopted to memory storage, it would exhibit a high power, since an infinite capacity of storage will be achieved in ideal case. In real circumstances, where a system is contaminated by various kinds of noise, an infinite capacity is impossible, but extremely high capacity is expected because of its robustness for noise. Actually, Cantor set itself survives in the direction of inhibitory neuron even in the noisy environment. One can assure this point in the figure of attractor and in the projected invariant measure to the direction of inhibitory neuron. This is a kind of realization of sophisticated use of Cantor code by Siegelmann and Sontag (1994).

It would be natural to ask the presence of SCND attractors in biological neural systems. Chaotic behaviors have been observed in several parts of brain. Thus, chaotic neurons or chaotic neural networks can act for higher functions of brain. On the other hand, non-chaotic, that is, static neurons or their networks also exist, and act for some information processings. Then, one can conceive the situation that a chaotic neuron or its network drives a static neuron or its network. Such a system will appear in cortical tissues that relate sensory information to feedback information from higher levels, that is, in "cortical interface". Among others, a significant candidate is a memory system which can be implemented in hippocampus and more widely in temporal cortex.

How can one detect such an attractor in brain ? According to the present study, the measurement of membrane potential of an inhibitory neuron, or local EEG of the network where inhibition is dominant, which should lie in the vicinity of the network exhibiting chaotic behaviors will provide an evidence of the existence of SCND attractors.

References

- Aihara, K., Takabe, T., and Toyoda, M. (1990). Chaotic neural networks, *Physics Letters A*, **144**, 333-340 .
- Freeman, W. J. (1987). Simulation of chaotic EEG patterns with a dynamic model of the olfactory system, *Biological Cybernetics*, **56**, 139-150.
- Freeman, W. J. (1994). Neural mechanisms underlying destabilization of cortex by sensory input, *Physica D*, **75**, 151-164.
- Freeman, W. J. (1995a). *Societies of Brains – A Study in the Neuroscience of Love and Hate* (Lawrence Erlbaum Associates, Inc., Hillsdale).
- Freeman, W. J. (1995b). Chaos in the brain: Possible roles in biological intelligence, *International Journal of Intelligent Systems*, **10**, 71-88.
- Grebogi, C., Ott, E., Pelikan, S., and Yorke, J. A. (1984). Strange attractors that are not chaotic, *Physica*, **13D**, 261-268.
- Hata, M. (1988a). On Weierstrass's non-differentiable function, *C.R. Academy of Science Paris*, **307**, 119-123.
- Hata, M. (1988b). Singularities of the Weierstrass type functions, *Journal d'Analyse Mathématique*, **51**, 62-90.
- Hata, M. (1994). Correction to "Singularities of the Weierstrass type functions", *Journal d'Analyse Mathématique*, **64**, 347.
- Hirsch, M. W. and Smale, S. (1974). *Differential Equations, Dynamical Systems and Linear Algebra* (Academic Press, New York 1974).
- Ikeda, K., Otsuka, K., and Matsumoto, K. (1989). Maxwell-Bloch turbulence, *Progress of Theoretical Physics, Supplement*, **99**, 295-324.
- Kai, T. and Tomita, K. (1980). Statistical mechanics of deterministic chaos, *Progress of Theoretical Physics*, **64**, 1532-1550.
- Kaneko, K. (1986). *Collapse of Tori and Genesis of Chaos in Dissipative Systems*, World Scientific, Singapore, p.118.
- Kaneko, K. (1990). Clustering, coding, switching, hierarchical ordering, and control in network of chaotic elements, *Physica D*, **41**, 137-172.

Kaplan, J. L. and Yorke, J. A. (1979). Chaotic behavior of multidimensional difference equations. *Lecture Notes in Mathematics*, **730**, 204-227.

Kaplan, J. L., Mallet-Paret, J., and Yorke, J. A. (1984). The Lyapunov dimension of nowhere differentiable attracting torus. *Ergodic Theory and Dynamical System*, **4**, 261-281.

Katsuura, H. (1991). Continuous nowhere-differentiable functions – an Application of Contraction Mappings, *American Mathematical Monthly*, **98**, 411-416.

Kay, L., Shimoide, K., and Freeman, W. J. (1995). Comparison of EEG time series from rat olfactory system with model composed of nonlinear coupled oscillators, *International Journal of Bifurcation and Chaos*, **5**, 849-858.

Mandelbrot, B. B. (1982). *The Fractal Geometry of Nature*, W. H. Freeman, San Francisco.

Matsumoto, K. and Tsuda, I. (1983). Noise-induced order. *Journal of Statistical Physics*, **31**, 87-106.

Matsumoto, K. and Tsuda, I. (1985). Information theoretical approach to noisy dynamics, *Journal of Physics A*, **18**, 3561-3566.

Matsumoto, K. and Tsuda, I. (1987). Extended information in one-dimensional maps, *Physica D*, **26**, 347-357.

Matsumoto, K. and Tsuda, I. (1988). Calculation of information flow rate from mutual information, *Journal of Physics A*, **21**, 1405-1414.

Moser, J. (1969). On a theorem of Anosov, *Journal of Differential Equations*, **5**, 411-440.

Rössler, O. E. and Hudson, J. L. (1984) A "superfat" attractor with a singular-continuous 2-D Weierstrass function in a cross section, *Zeitschrift für Naturforschung*, **48a**, 673-678.

Rössler, O. E., Wais, R., and Rössler, R. (1992). Singular-continuous Weierstrass function attractors, In *Proceedings of the 2nd International Conference on Fuzzy Logic and Neural Networks*, (Iizuka, Japan) 909-912.

Rössler, O. E., Hudson, J. L., Knudsen C., and Tsuda, I. (1995). Nowhere-differentiable attractors, *International Journal of Intelligent Systems*, **10**, 15-23.

Siegelmann, H. and Sontag, E. D. (1994). Analog computation via neural networks, *Theoretical Computer Sciences*, **131**, 331-360.

- Takagi, T. (1973). A simple example of the continuous without derivative, in *The Collective Papers of Teiji Takagi*, Iwanami Shoten Publ., Tokyo.
- Titchmarsh, E. C. (1985). *The Theory of Functions*, Oxford Univ. Press.
- Tsuda, I., Körner, E., and Shimizu, H. (1987). Memory dynamics in asynchronous neural networks, *Progress of Theoretical Physics*, **78**, 51-71.
- Tsuda, I. (1991a). Chaotic neural networks and Thesaurus, *Neurocomputers and Attention I* (eds., A. V. Holden and V. I. Kryukov, Manchester University Press, Manchester), 405-424.
- Tsuda, I. (1991b). Chaotic itinerancy as a dynamical basis of Hermeneutics of brain and mind, *World Futures*, **32**, 167-185.
- Tsuda, I. (1992). Dynamic link of memories—chaotic memory map in nonequilibrium neural networks, *Neural Networks*, **5**, 313-326.
- Tsuda, I. (1994). Can stochastic renewal of maps be a model for cerebral cortex? *Physica D*, **75**, 165-178.
- Tsuda, I. (1996). A new type of self-organization associated with chaotic dynamics in neural systems. *International Journal of Neural Systems* (to appear).
- Yamaguti, M. (1989). Schauder expansion by some quadratic base function, *Journal of the Faculty of Science, The University of Tokyo, secIA*, **36**, 187-191.
- Yamaguti, M. and Hata, M. (1984). Takagi function and its generalization, *Japan Journal of Applied Mathematics*, **1**, 186-199.

Table captions

Table 1 Lyapunov spectrum and Lyapunov dimension for some typical values of b .

Figure captions

Fig. 1 Neuron models adopted in this paper: (a) for a static neuron, and (b) for a dynamic one.

Fig. 2 Cantor set attractors seen on a cross section $x = 0.05 (\pm 0.0005)$: (a) $b = 0.93$, (b) $b = 0.95$, and (c) $b = 0.99$.

Fig. 3 Return map of Y taken on the cross section for $b = 0.93$.

Fig. 4 Invariant measure computed in $Y - Z$ plane. The orbits on the cross section are used. A mesh size for coarse-graining is given by 30×30 partitions.

Fig. 5 Comparison of invariant measure ((a)) with $\tau(X_r^*, X)^{-1}$ ((b)) and $\tau(X_l^*, X)^{-1}$ ((c)) in isolated chaotic map.

Fig. 6 Exponent $\nu(X)$ as a function of X . This exponent gives a good approximation of invariant measure.

Fig. 7 Lyapunov dimension *v.s.* contraction parameter b .

Fig. 8 Noise-induced order represented by conditional entropy. The case of $b = 0.93$ is shown, but this noise effect is observed also in other parameter values as far as SCND attractors appear.

Fig. 9 The dependence of the number of bins including at least one data point on noise amplitude.

Fig. 10 Noise-induced order represented by mutual information. This is a general character of SCND attractors in the same sense as mentioned for conditional entropy.

Nomenclature

x_n , y_n , and z_n : neuron's output, that is, pulse density per unit time at time n .

$f_i(x)$: sigmoidal function expressing input-output relation of neuron.

X_n , Y_n , and Z_n : neuron's internal state expressing membrane potential of neuron at time n .

X'_n , Y'_n , and Z'_n : neuron's internal state at time $n - 1$.

b_i : decay rate of internal memory.

c_{ij} : synaptic strength from neuron i to j .

$F(X_n)$: transformation function of membrane potential.

D : unit square.

$H(D)$: collection of all nonempty closed subsets of D .

$K(A)$, and $R(A)$: contraction map for area A .

f_n , and g_n : function on unit interval.

L_n , and S_n : graph of function.

D : Dini's derivative.

dim_h : Hausdorff dimension.

dim_t : topological dimension.

$\tau(u, v)$: time from u to v .

$P_X(T)$: distribution of recurrence time T on the cross section X .

$\nu(X)$: exponent of the recurrence time distribution on X .

$H(U'/U)$: conditional entropy of U' under the condition U .

p_i : stationary probability distribution.

p_{ij} : transition probability distribution from i to j .

Δ : difference between two distributions.

$I(t)$: time-dependent mutual information.

I : stationary mutual information.

	λ_1	λ_2	λ_3	λ_4	λ_5	λ_6	Lyapunov dimension
$b = 0.93$	0.22	-0.27	-0.27	-2.44	-2.54	-33.54	1.82
$b = 0.94$	0.23	-0.24	-0.24	-2.56	-2.66	-33.50	1.97
$b = 0.95$	0.37	-0.20	-0.20	-2.72	-2.75	-33.08	2.76
$b = 0.96$	0.42	-0.17	-0.17	-2.90	-2.91	-32.79	3.03
$b = 0.98$	0.42	-0.10	-0.10	-3.46	-3.46	-32.52	3.06
$b = 0.99$	0.44	-0.05	-0.05	-4.02	-4.02	-31.98	3.08

Table 1

Tsuda et al

(a)

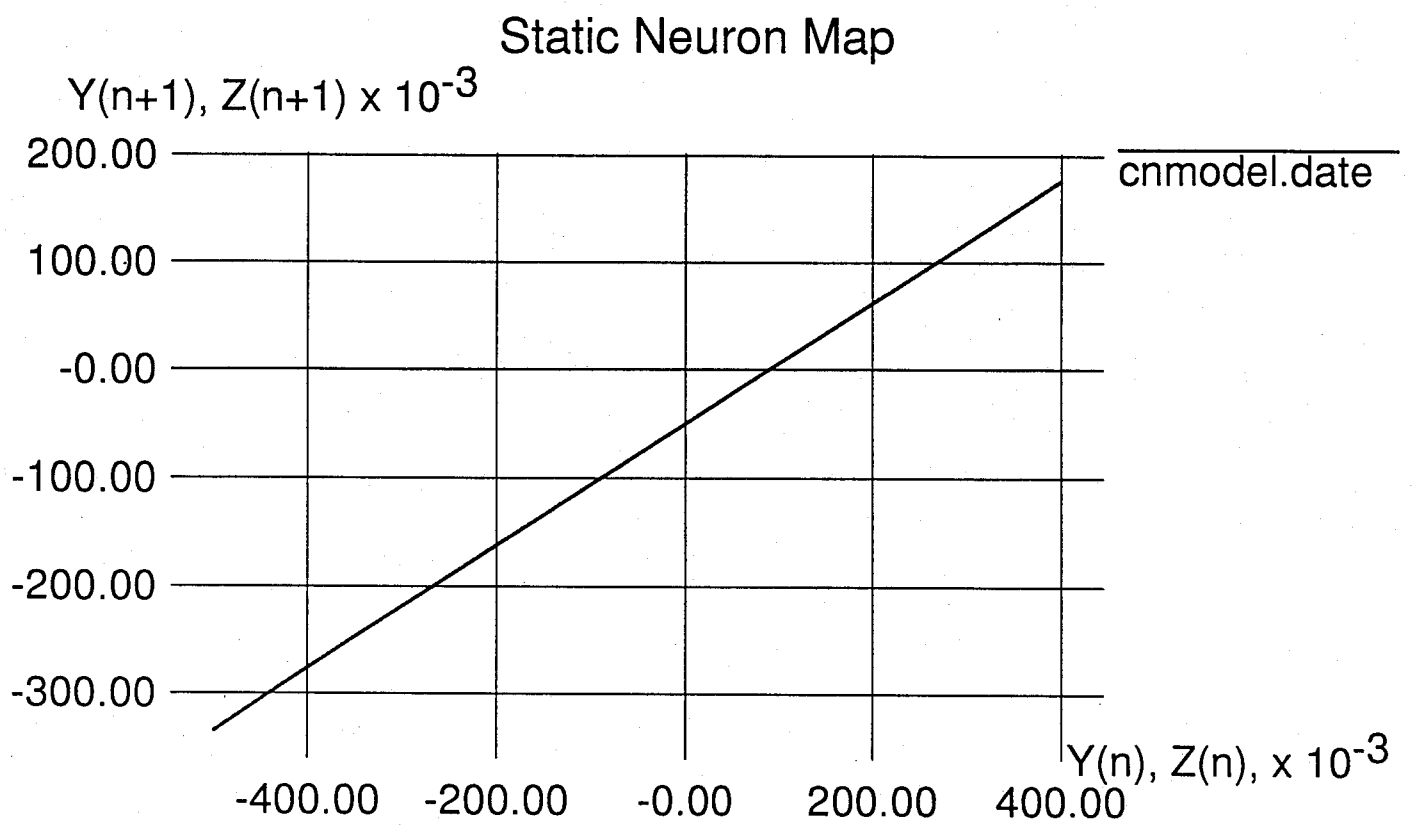


Fig 1. (a)

Tsuda et al

(b)

Chaotic Neuron Map

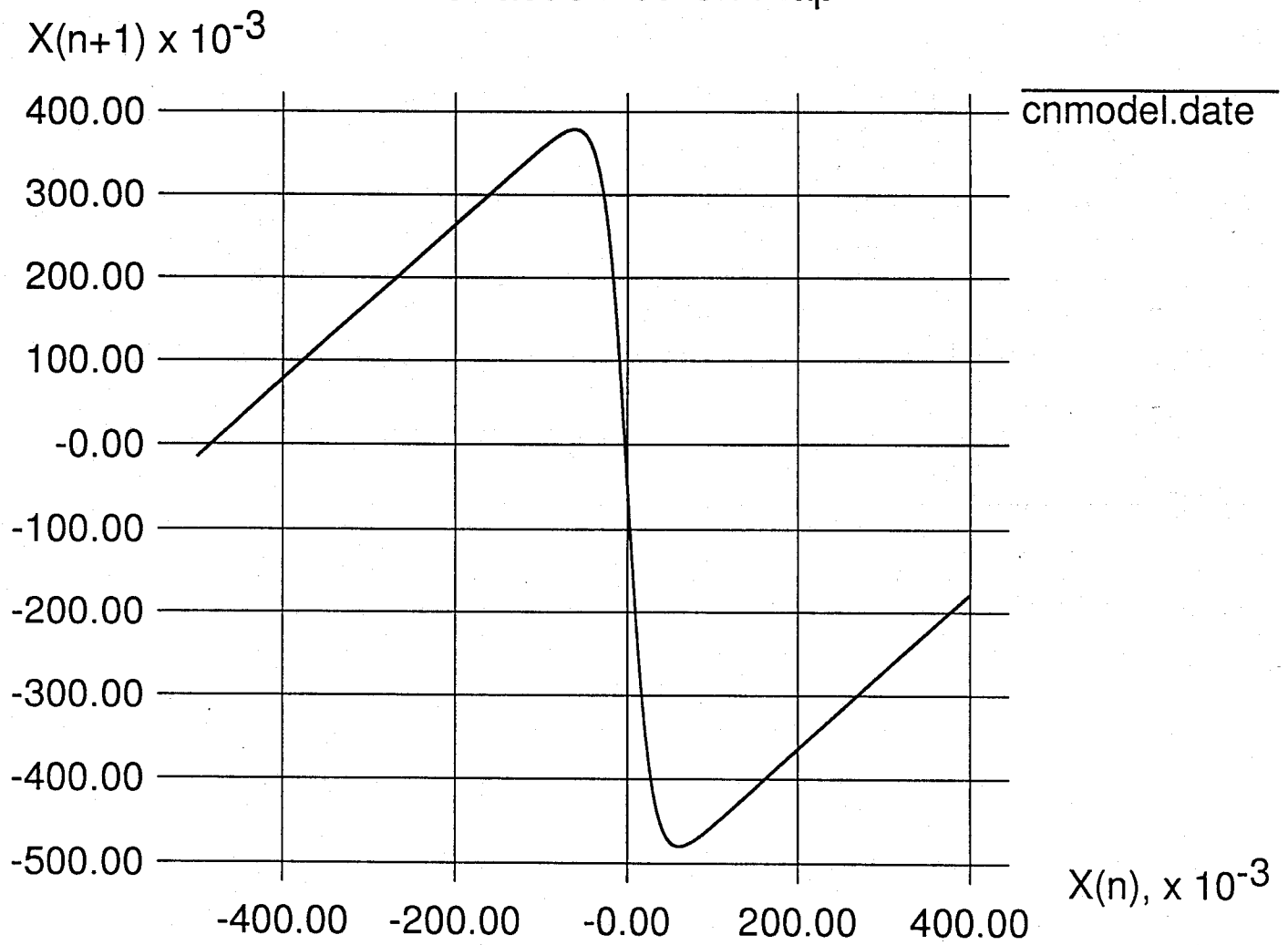


Fig 1 (b)

Tsuda et al

(a)

Z

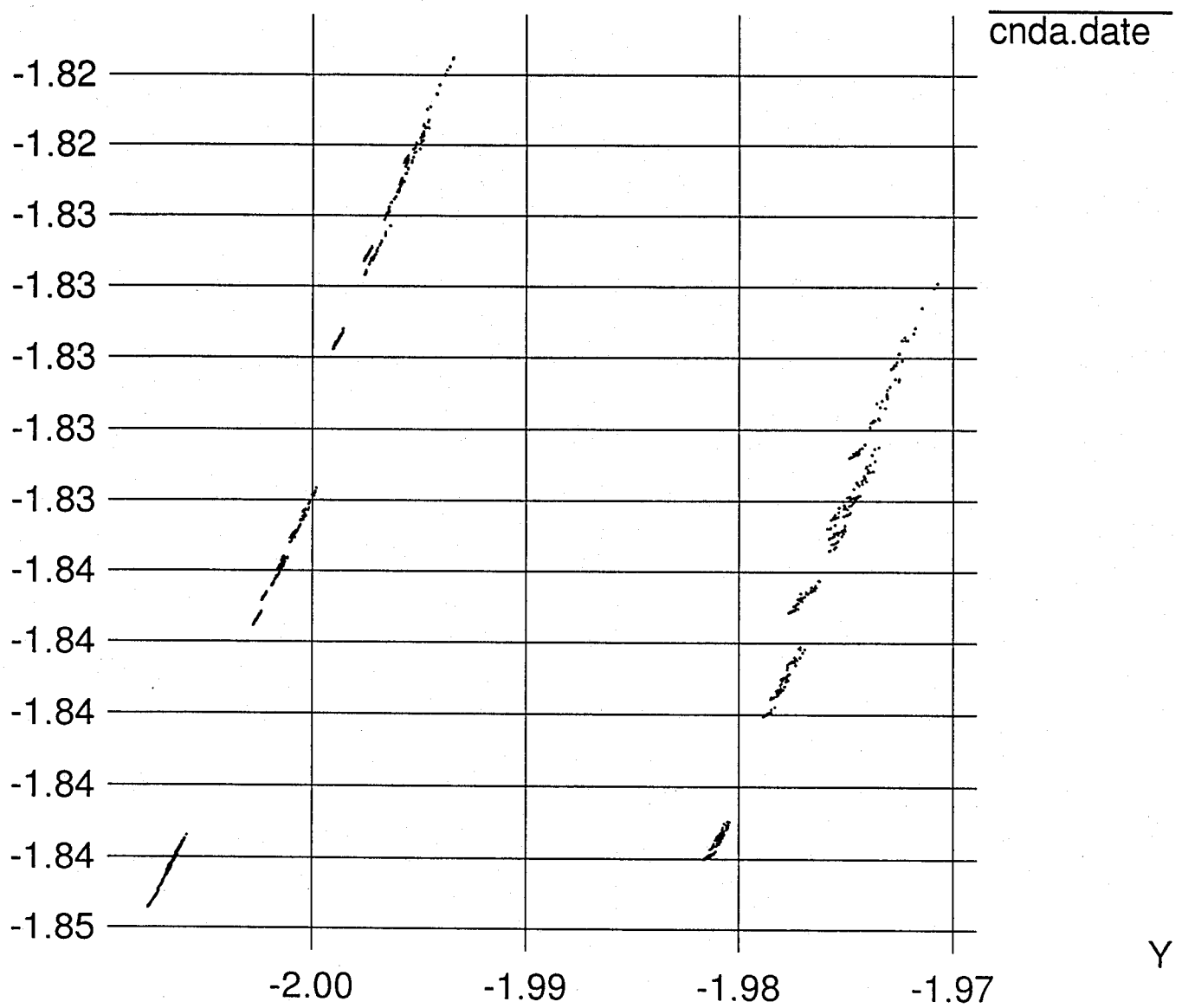
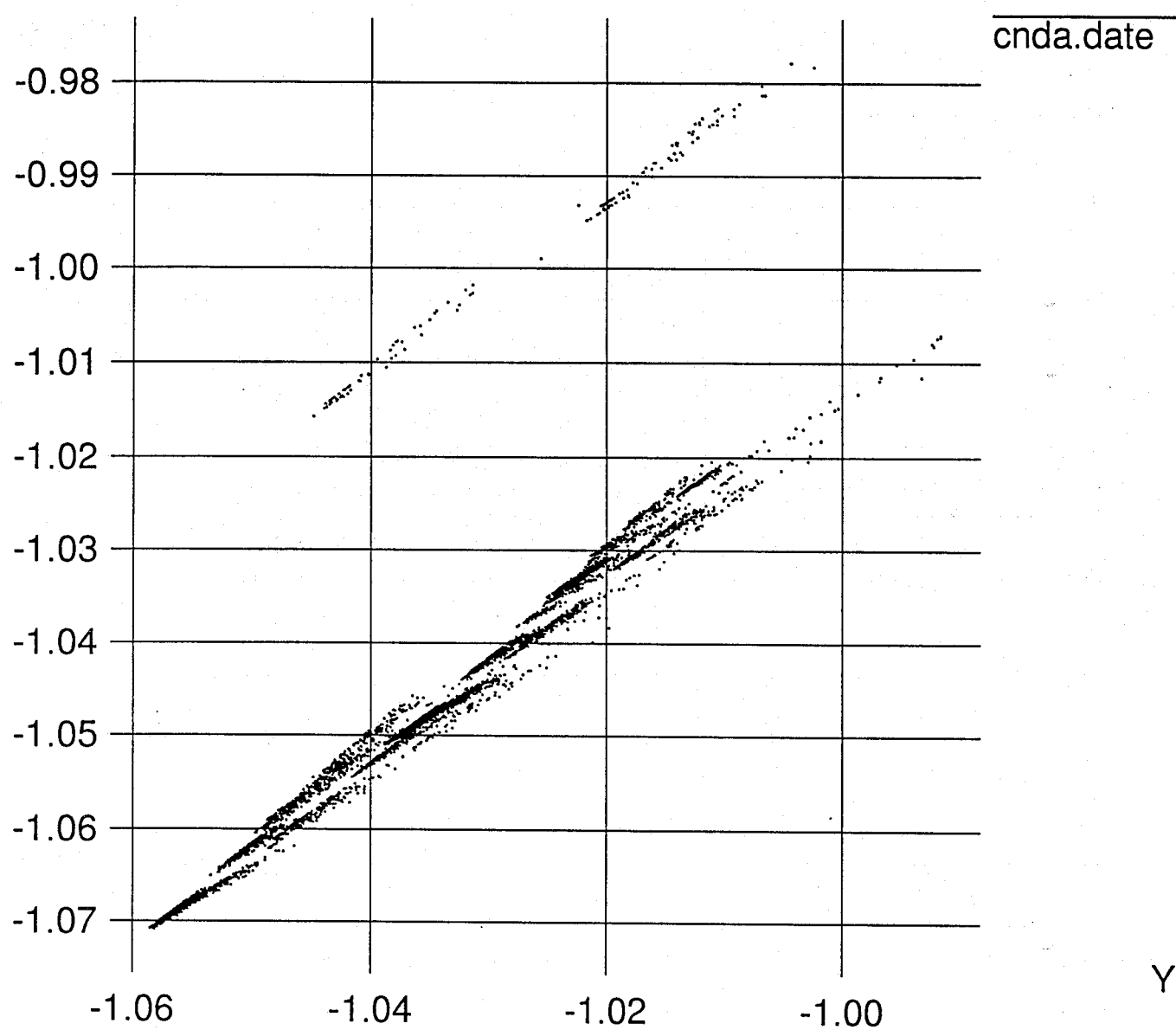


Fig 2 (a)

Tsuda et al

(b)

Z



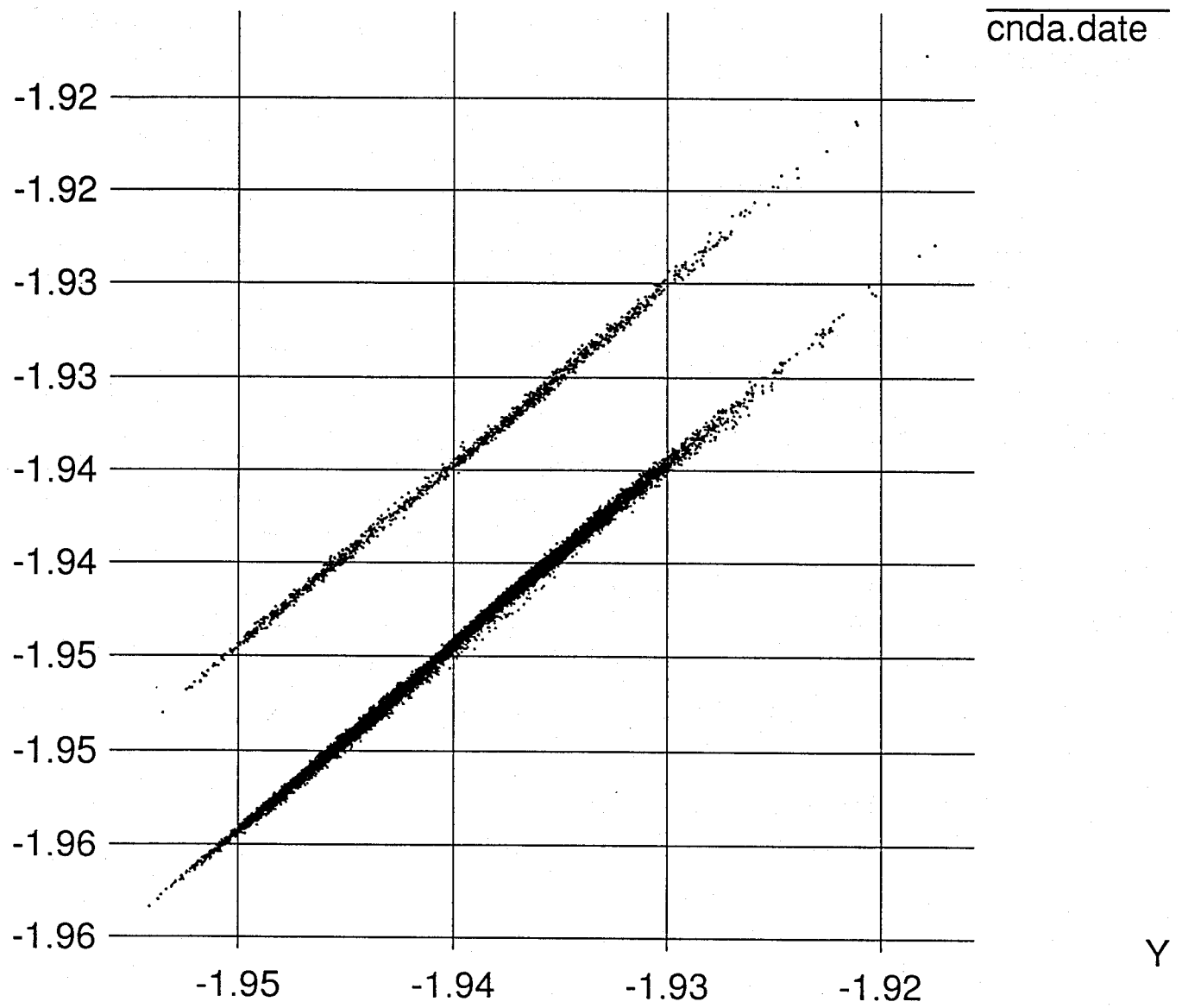
Y

Fig 2 (b)

Tsuda et al

(c)

Z



Y

Fig 2 (c)

Tsuda et al

$Y(n+1)$

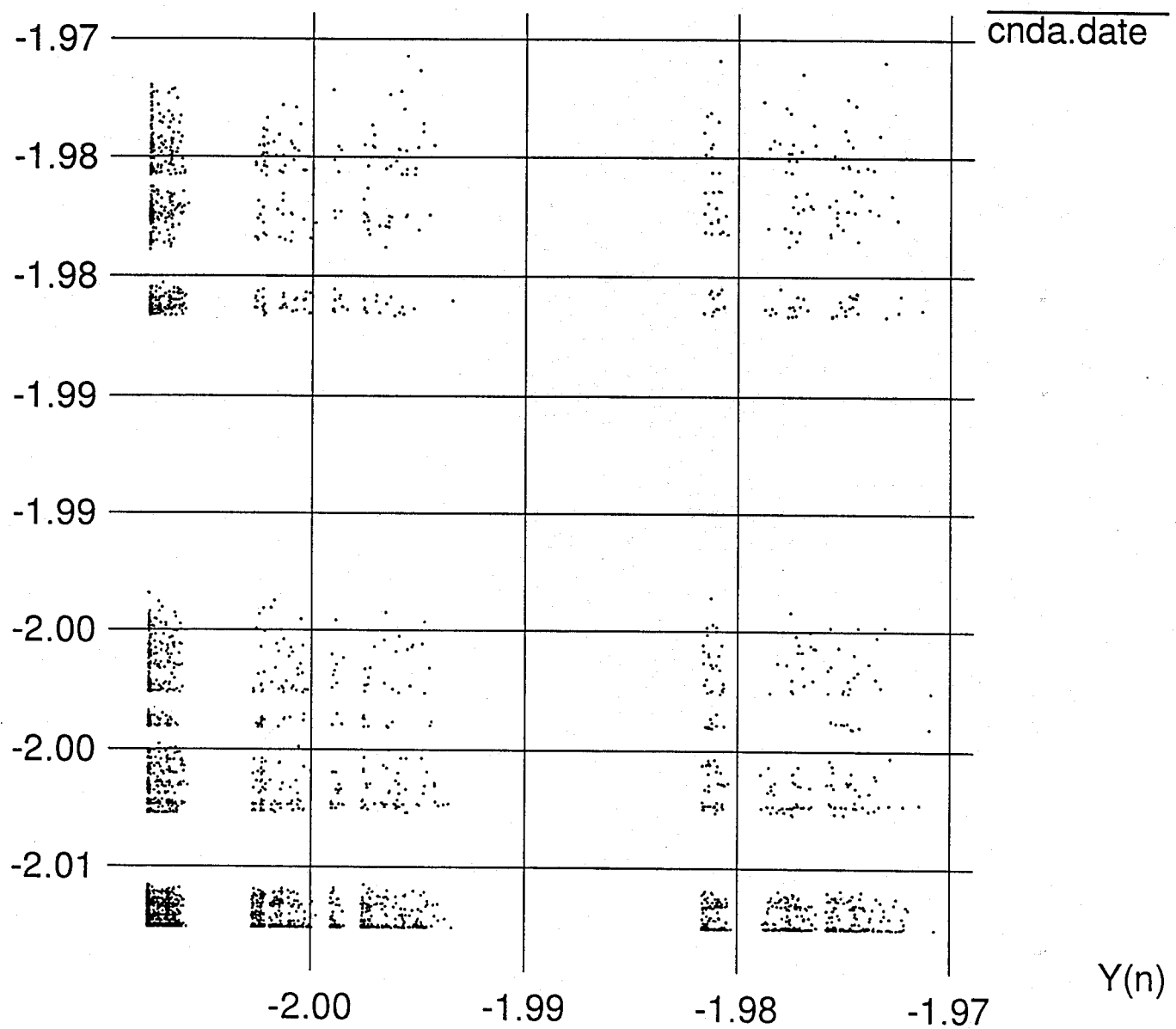


Fig. 3

Tsuda et al

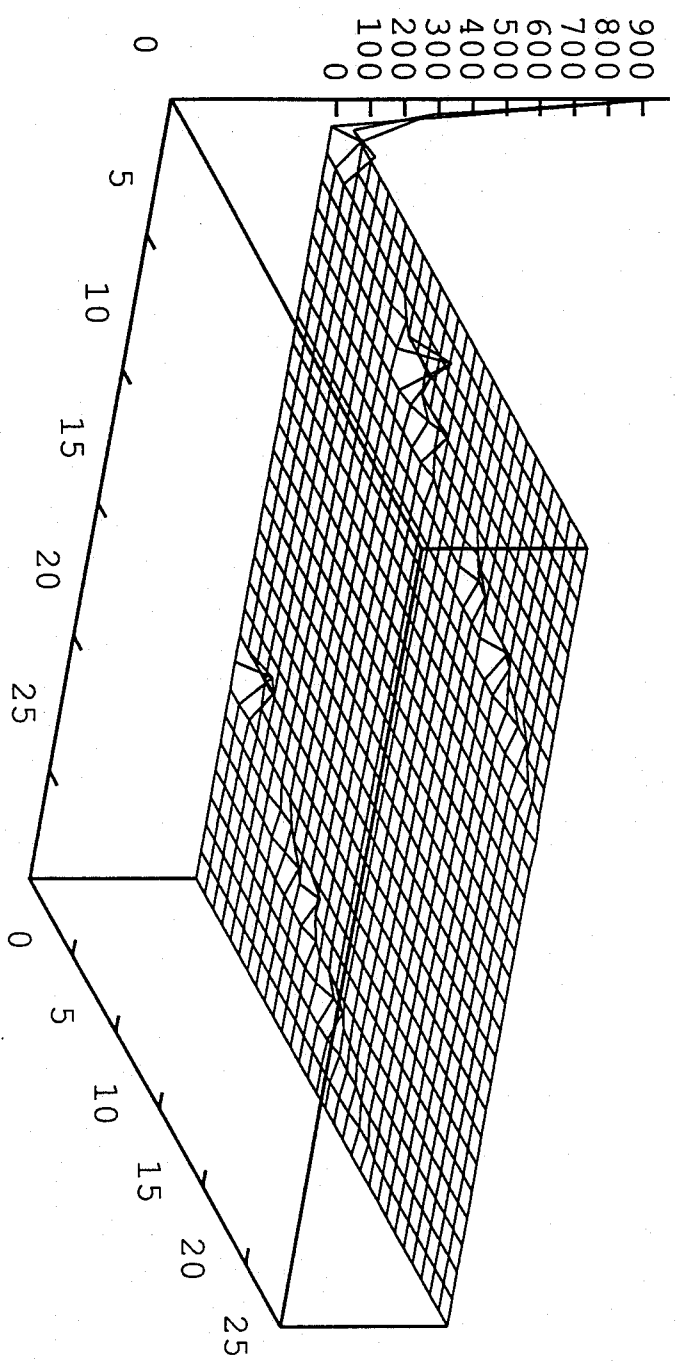


Fig 4. Tsuda et al

(a)

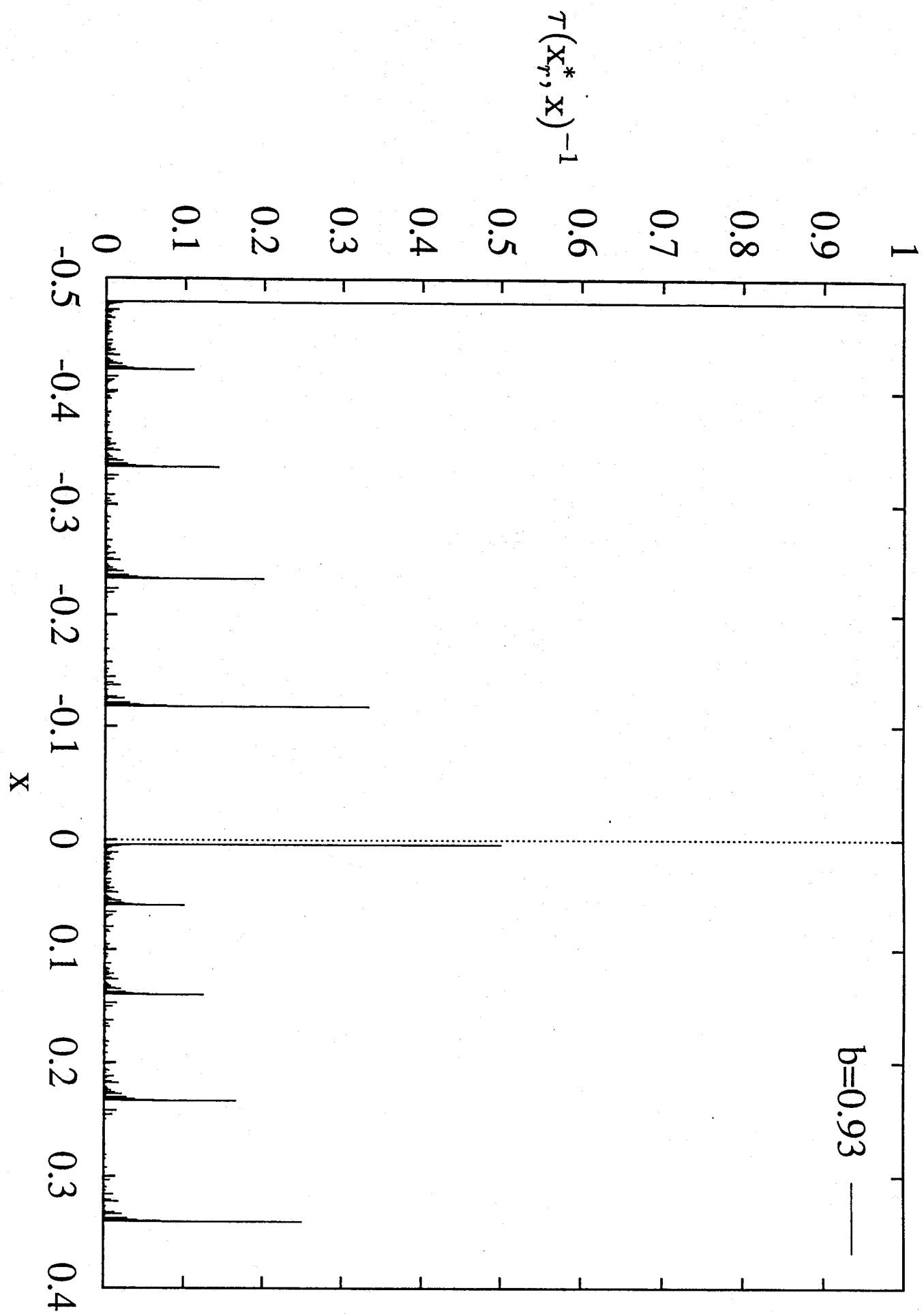


Fig 5(a)
Tsuda et al

(b)

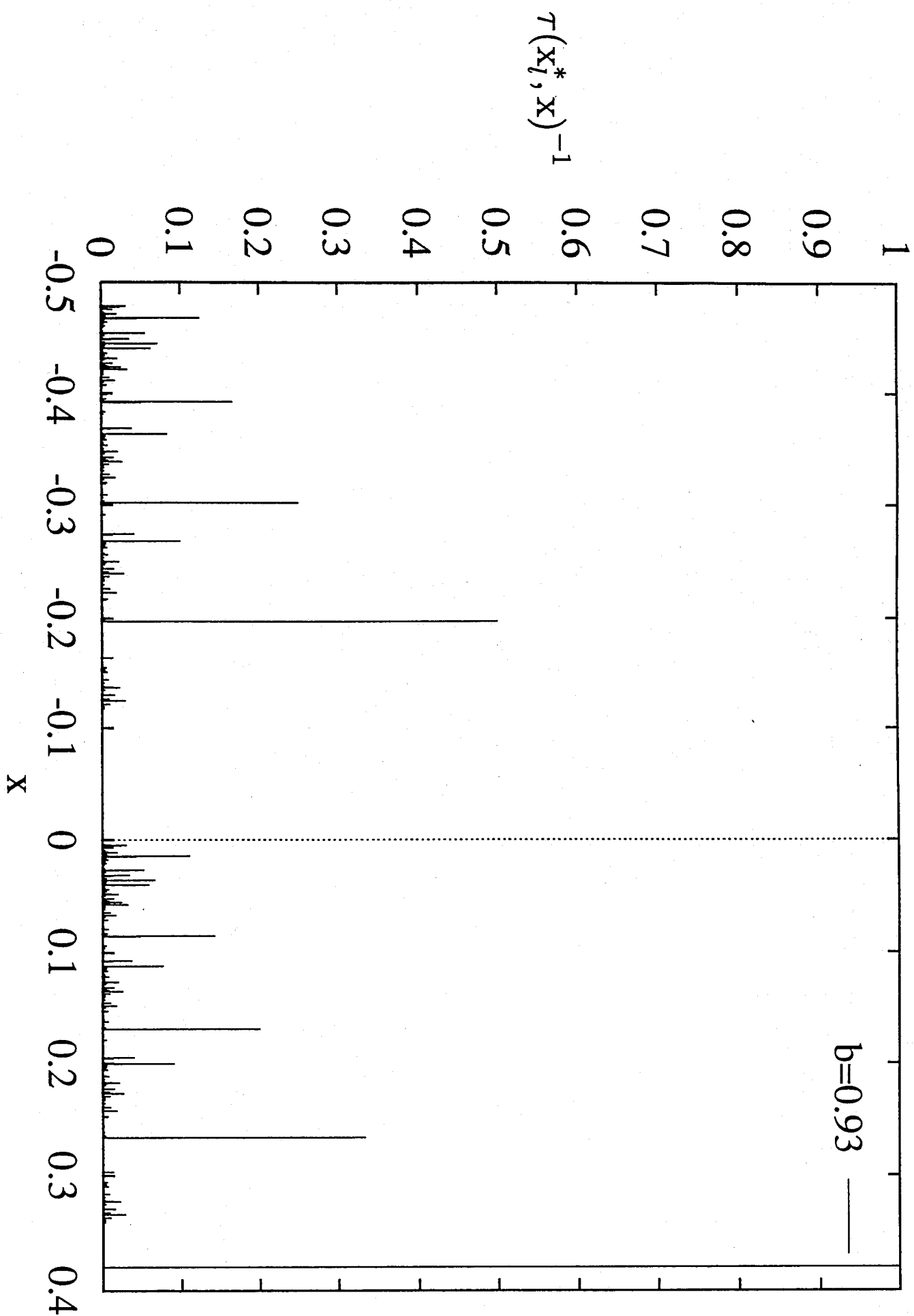


Fig 5(b)
Tsuda
et al

(c)

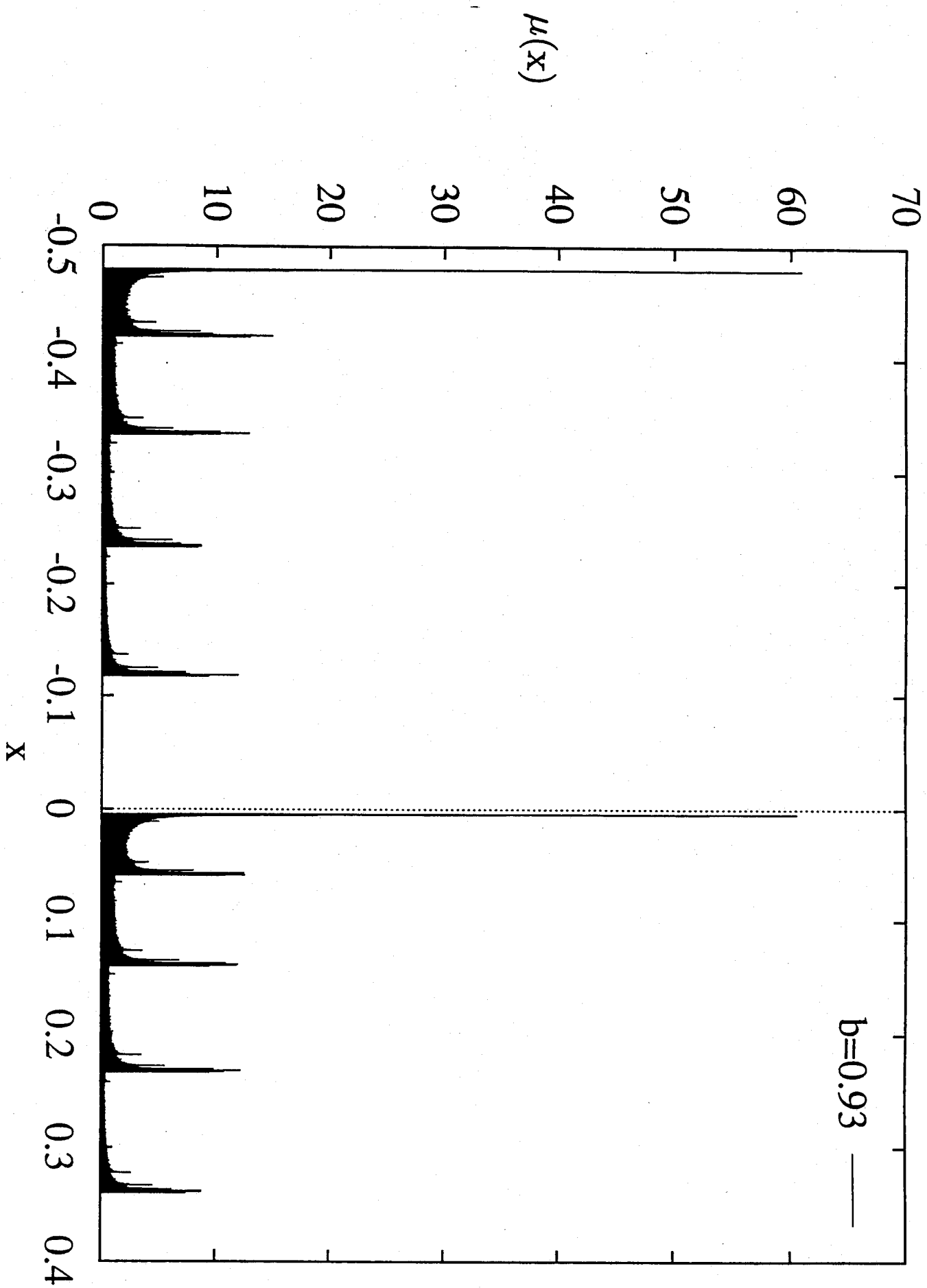


Fig 5(c)
Tsuda
et al

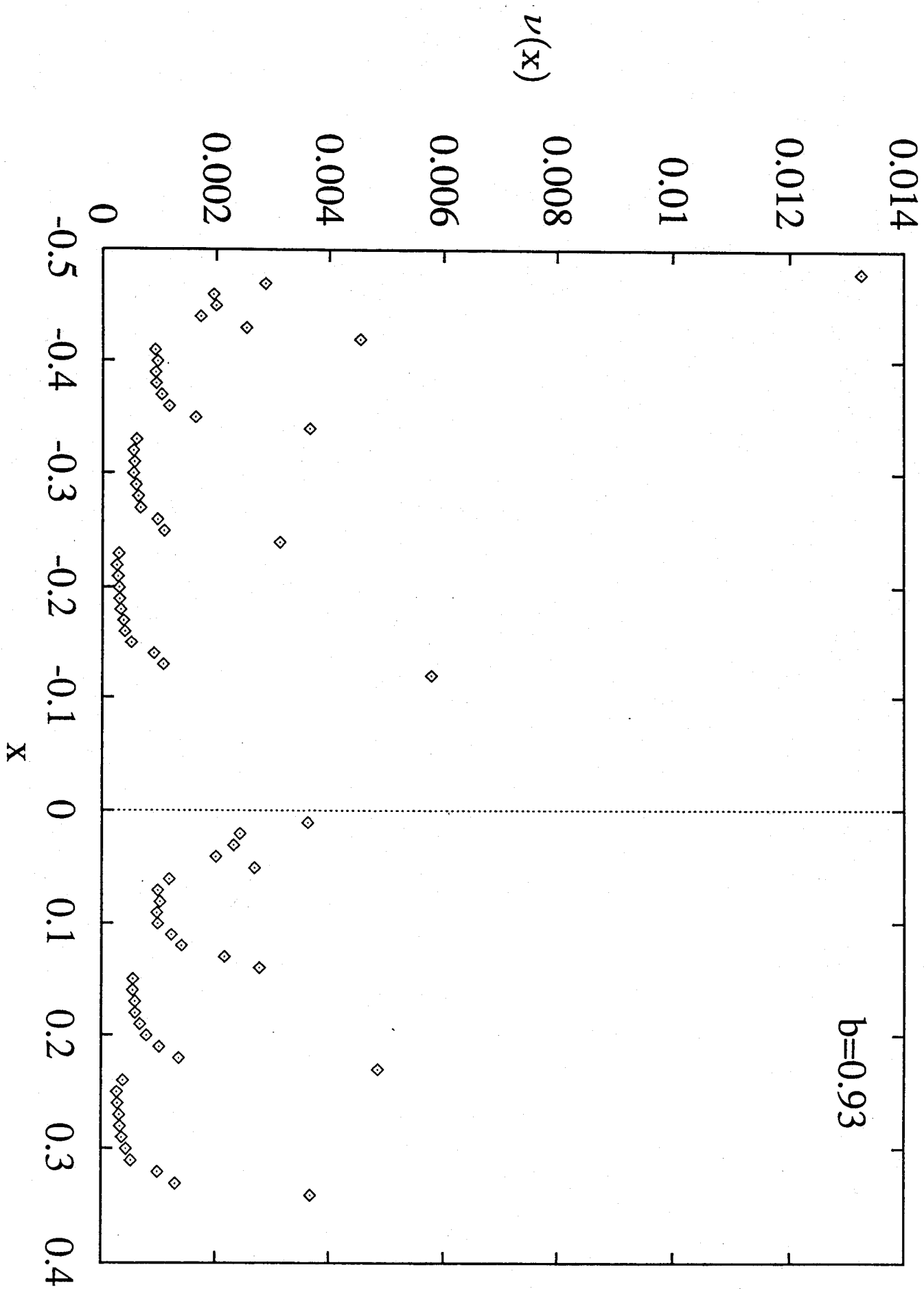


Fig 6
Tsuchida
et al

Lyapunov dimension v.s. parameter (b)

dim.

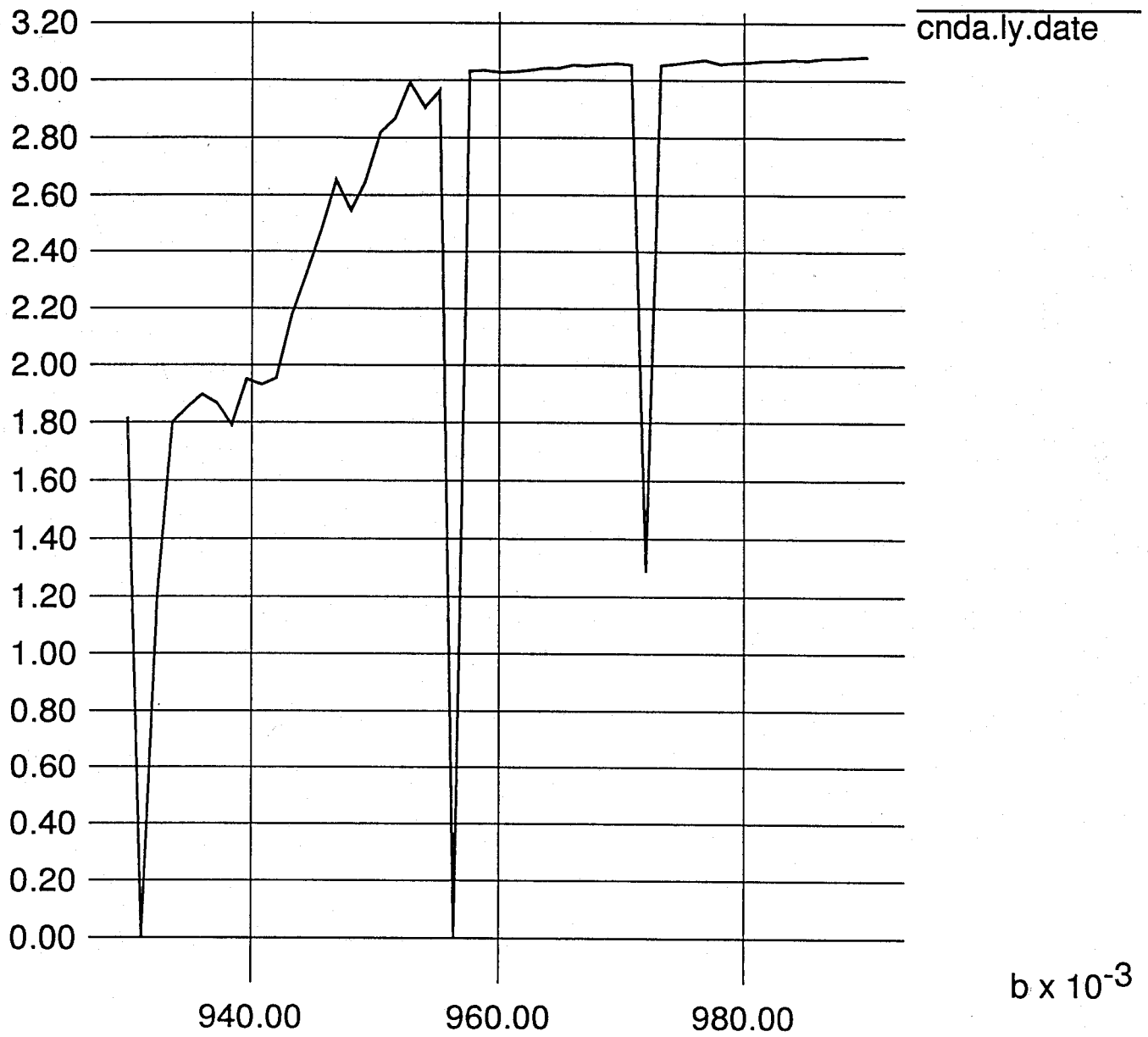
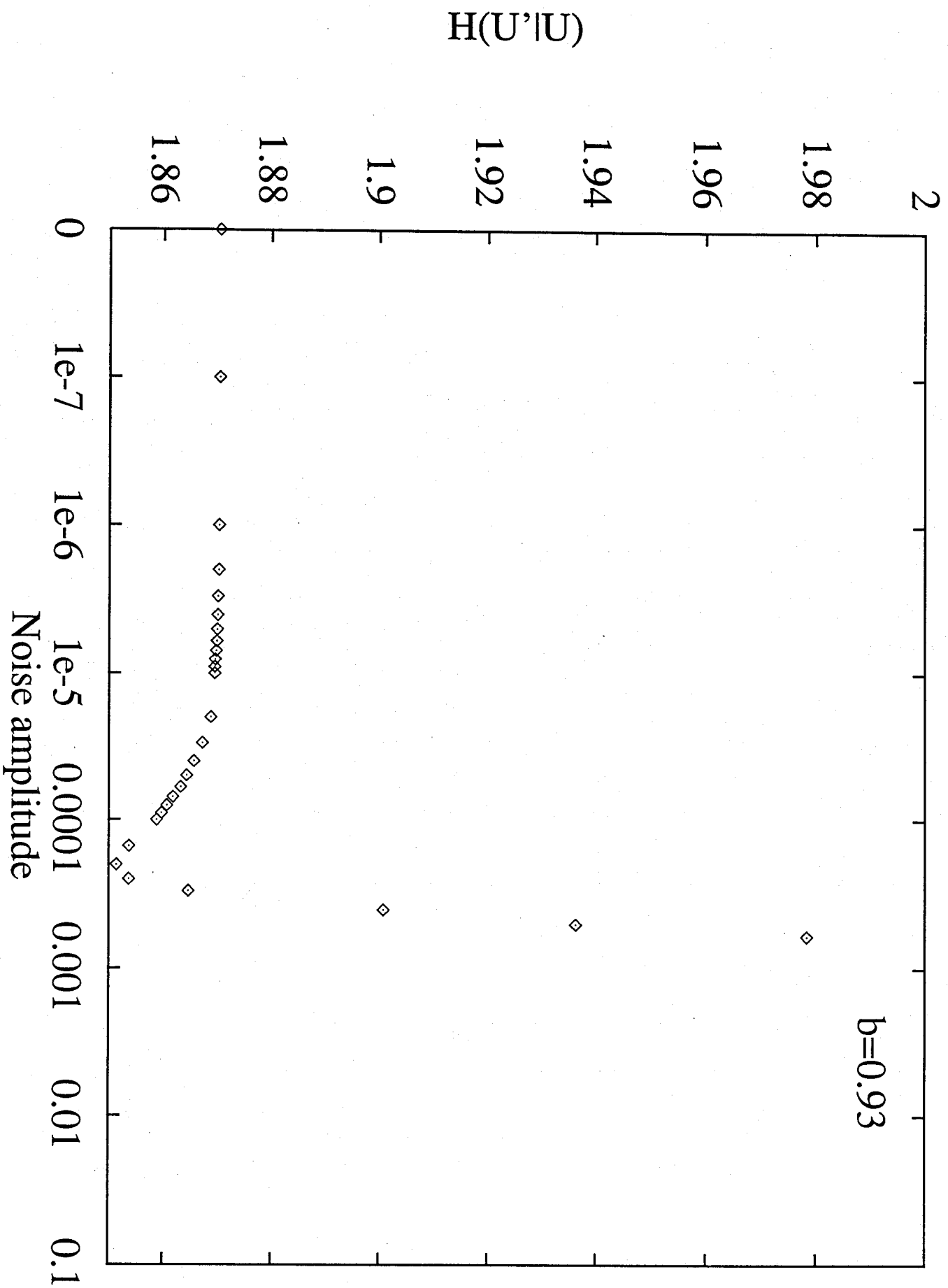


Fig. 7

Tsuda et al



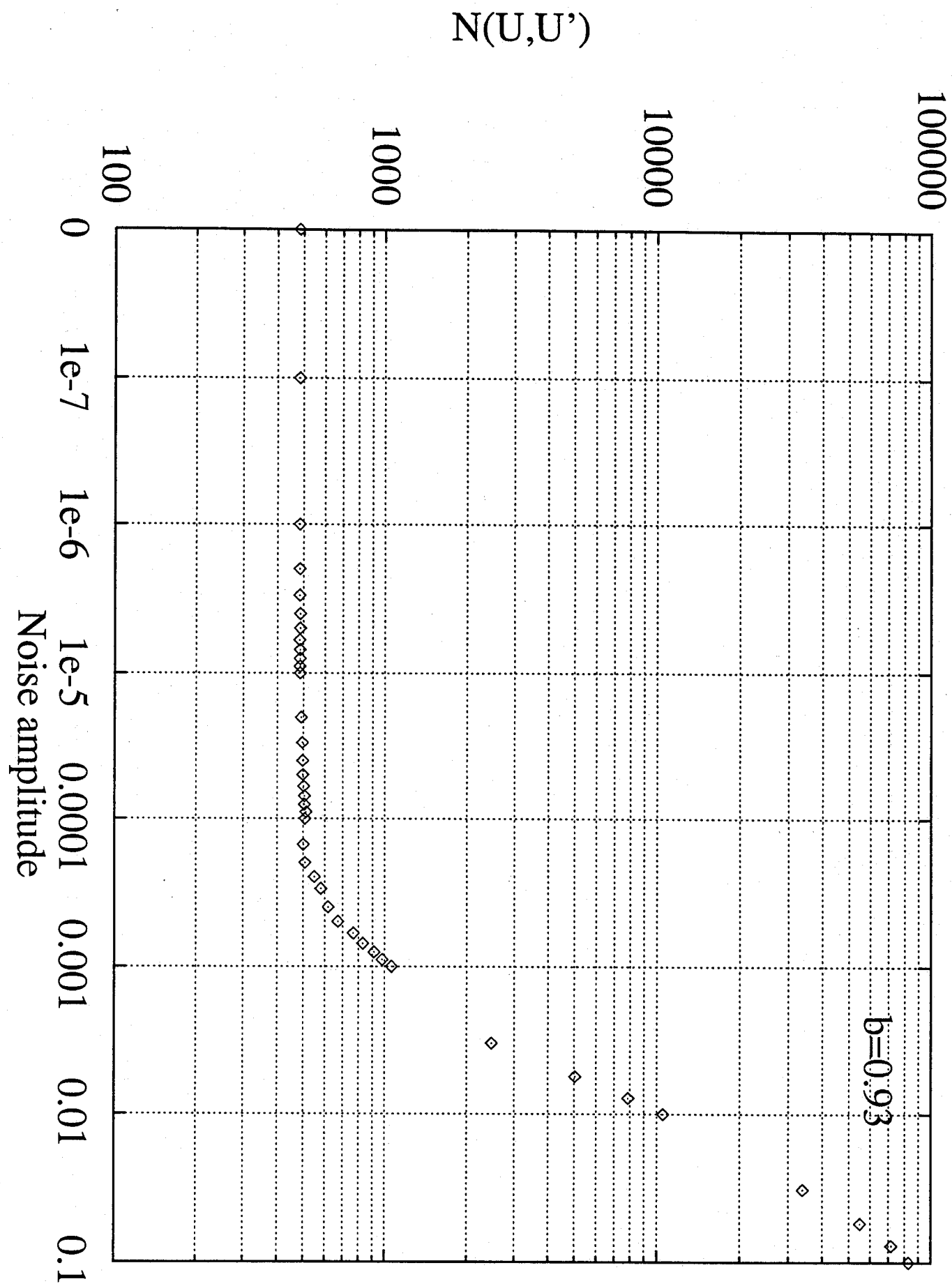


Fig 9
 T_{std}
std

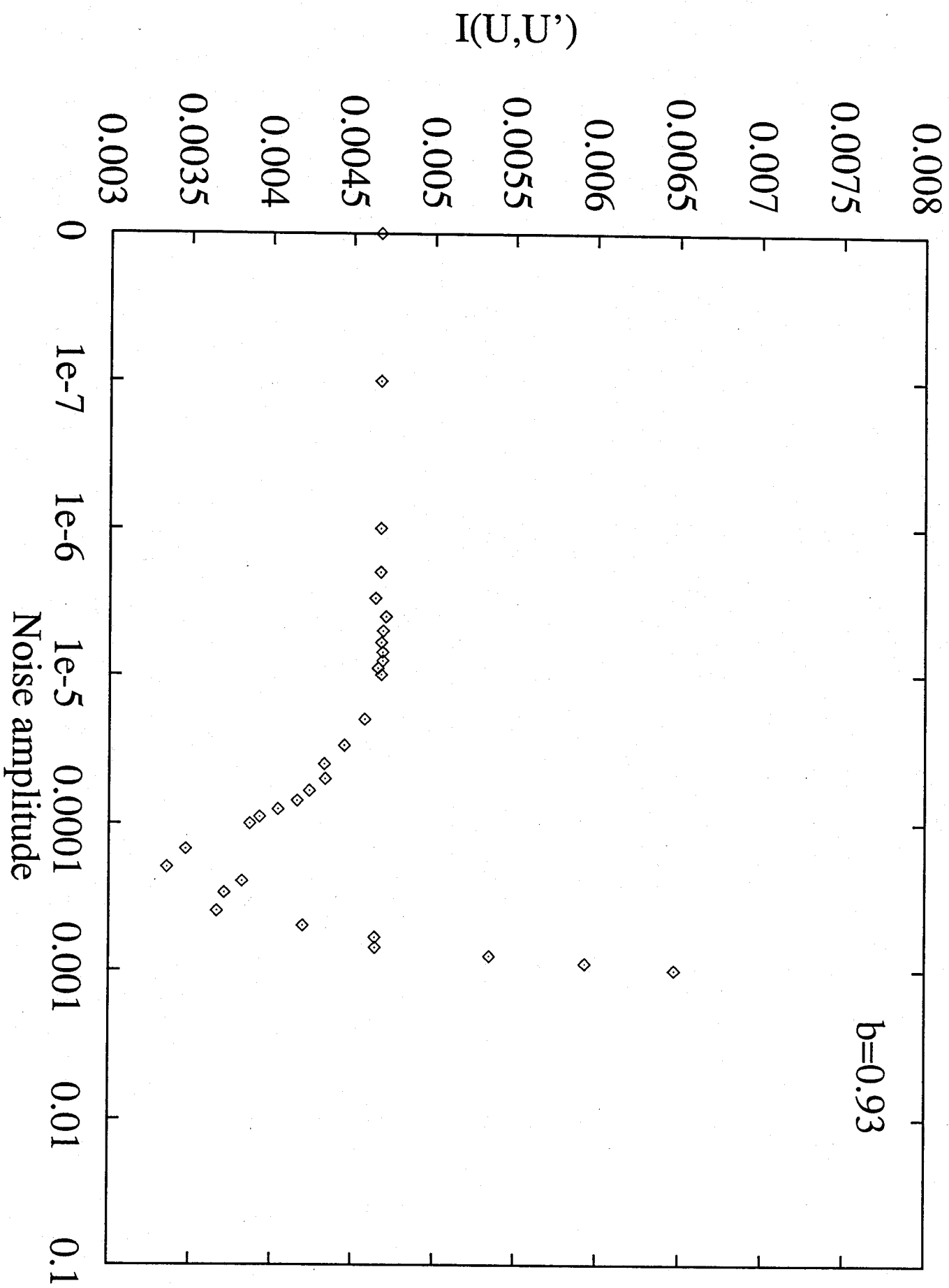


Fig. 10
 T_{rad}
and